HHS Public Access

Author manuscript

Clin Imaging. Author manuscript; available in PMC 2016 February 14.

Published in final edited form as:

Clin Imaging. 2015 ; 39(5): 787–790. doi:10.1016/j.clinimag.2015.05.015.

Hypertrophic olivary degeneration resulting from posterior fossa masses and their treatments☆,,☆☆,,★

Miki Hirano[a], **Vaios Hatzoglou**[a,b], **Sasan Karimi**[a,b], and **Robert J. Young**[a,b,*]

Miki Hirano: mikihirano89@gmail.com; Vaios Hatzoglou: hatzoglv@mskcc.org; Sasan Karimi: karimis@mskcc.org; Robert J. Young: youngr@mskcc.org

[a]Department of Radiology, Memorial Sloan Kettering Cancer Center, New York, New York

[b]Brain Tumor Center, Memorial Sloan Kettering Cancer Center, New York, New York

Abstract

Purpose—Characterize hypertrophic olivary degeneration (HOD) that develops from posterior fossa masses and their treatments.

Methods—Retrospectively reviewed MR images and clinical data of 10 patients with posterior fossa masses and HOD.

Results—Eight patients had cerebellar lesions, and two patients had pontine lesions. Lesions consisted of tumors, demyelination, and nonspecific necrosis. MRI showed T2 hyperintense signal in the inferior olive a median 86 days after the diagnosis of a posterior fossa lesion. HOD presented prior to surgery (*n*=2), after surgery (*n*=3), after surgery/radiation therapy (*n*=4), or without treatment (*n*=1).

Conclusions—HOD may develop from posterior fossa masses and surgical and/or radiation therapy.

Keywords

MRI; All oncology; Radiation-therapy tumor; Surgical-therapy tumor

1. Introduction

Hypertrophic olivary degeneration (HOD) was first reported by Oppenheim in 1887 and confirmed by multiple authors in 1902 and 1903 [1]. HOD presents at MRI with abnormal T2-hyperintense signal in the inferior olive that may be accompanied by abnormal hypertrophy of the olive. HOD occurs with lesions in the Guillain-Mollaret or dento-rubro-olivary triangle, which consists of the connection between the red nucleus, ipsilateral inferior olivary nucleus, and contralateral dentate nucleus [2,3]. The dentatorubral tract

☆Funding: Miki Hirano was supported by a Medical Student Summer Fellowship from the Brain Tumor Center of Memorial Sloan Kettering Cancer Center.

☆☆Authorship: Design and conceptualization of the study (SK, RJY), analysis and interpretation of the data (MK, VH, SK, RJY), drafting and revising the manuscript (MK, VH, SK, RJY), and final approval of submitted version (MK, VH, SK, RJY).

★Financial disclosures: All authors report no disclosures.

*Corresponding author. Memorial Sloan Kettering Cancer Center, 1275 York Avenue, New York, New York, 10065. Tel.: +1-212-639-8196; fax: +1-917-432-2345.

connects the dentate nucleus to the contralateral red nucleus. The central tegmental tract connects the red nucleus to the ipsilateral inferior olive. A lesion to either of these afferent tracts results in HOD. A lesion to the third and only efferent limb traversing the inferior cerebellar peduncle does not result in HOD. HOD is unique in that the trans-synaptic olivary degeneration results in swelling rather than shrinking [2–5]. Patients may present with palatal or dentate-rubral myoclonus. The majority of studies have described HOD resulting from posterior fossa hemorrhage or infarction. HOD in patients with brain tumors and tumor-like masses has not been well characterized. The purpose of this study was to evaluate HOD that develops from posterior fossa masses and their treatments.

2. Materials and methods

2.1. Standard protocol approvals, registrations, and patient consents

A waiver of informed consent was obtained from the local institutional review board. This study was compliant with local privacy board and all Health Insurance Portability and Accountability Act regulations.

2.2. Patients

We conducted a retrospective text-based search of radiology reports from a departmental database from January 1997 to June 2013. Search parameters included “hypertrophic olivary degeneration,” “olivary degeneration,” “hypertrophic olive,” “inferior olive,” and “HOD.” The diagnosis of HOD was defined as (a) abnormal T2 hyperintensity and/or enlargement of the inferior olive by MRI and (b) inciting lesion in an afferent limb of the Guillain-Mollaret triangle. The database query yielded 13 patients, with 2 patients excluded because of insufficient imaging and 1 patient excluded because there was no apparent lesion in the Guillain-Mollaret triangle. One patient with HOD complicated by radiation injury was previously reported [6]. We performed chart reviews of the 10 cohort patients (3 women and 7 men; range, 5–67 years; median age, 44 years) and collected clinical data from radiation oncology, pathology, and radiology records.

2.3. Imaging

The standard brain MRI protocol included sagittal and axial T1-weighted images; axial T2-weighted, fluid attenuated inversion recovery, diffusion weighted, and gradient echo or susceptibility weighted images; and gadolinium- enhanced coronal, sagittal, and axial T1-weighted images. An attending neuroradiologist with 7 years of experience reviewed all available brain MRI examinations. The presence of HOD was recorded when T2 hyperintense signal±hypertrophy was found in the inferior olive without enhancement or diffusion restriction [2,7]. The location of the lesion(s) in the Guillain-Mollaret triangle was recorded, and hemorrhage was evaluated from gradient echo (n=1), susceptibility weighted (n=2), b0 diffusion weighted (n=6), and noncontrast computed tomography (n=1) images.

Diffusion tensor imaging (DTI) was available in four patients (Pts. 3, 4, 6, and 8). Single-shot spin-echo echo-planar images were acquired in 15 noncollinear directions and b=1000 s/mm^2. Analysis was performed using nordicBrainEx v1.1.3 (NordicNeuroLabs, Milwaukee, WI, USA). Motion and eddy current corrections were applied and fractional anisotropy (FA)

and directionally encoded color FA maps calculated. Streamline tractography was performed with termination criteria of FA<0.15 and turning angle >60°.

3. Results

Patients had unilateral cerebellar lesions (*n*=4, developed contralateral HOD), midline cerebellar lesions (*n*=4, developed bilateral HOD), or unilateral pontine lesions (*n*=2, developed ipsilateral HOD). Lesions consisted of primary tumors (*n*=7), metastasis (*n*=1), tumefactive demyelination (*n*=1), and nonspecific necrosis (*n*=1), as summarized in Table 1. Lesion diagnosis was established by gross resection (*n*=6), biopsy (*n*=3), or follow-up (*n*=1, one patient with demyelination based on cerebrospinal fluid analysis and improvement with steroid treatment). Hemorrhage was present in four lesions before any intervention. The most common complaint was of nystagmus (*n*=7), followed by ataxia (*n*=5), dysphagia (*n*=3), and diplopia (*n*=1). Four patients had symptoms before the imaging diagnosis of HOD (median, 87 days) and four patients after the imaging diagnosis of HOD (median, 29 days).

MRI showed T2 hyperintense signal in the inferior olive a median interval of 86 days (range, 0–363) after diagnosis of the posterior fossa lesion. HOD was present prior to surgery in two patients. This includes HOD diagnosis at the time of lesion diagnosis in 1 patient (Pt 1). Most of the patients (*n*=9) had scans every 2–4 months during follow up, aside from a glioblastoma patient who did not have a postoperative MRI until 363 days later. Seven patients (70%) were diagnosed with HOD a median of 86 days after surgery for their posterior fossa mass (range, 6–363 days). From these seven patients, four patients had also completed radiation therapy (RT) a median interval of 71 days (range, 28–288) prior to HOD (doses of 5760–6000 cGy). The last patient (Patient 6) never underwent surgery or RT.

DTI in four patients suggested decreased anisotropy and fiber tracts in an afferent limb of the Guillain-Mollaret triangle at the level of the central tegmental tract (*n*=2, ipsilateral HOD) (Fig. 1) or the superior cerebellar peduncle (*n*=2, contralateral HOD) (Fig. 2).

4. Discussion

We describe HOD in 10 patients with posterior fossa masses, and based on the timing of their diagnoses and treatments, postulate the causes of trans-synaptic denervation of the inferior olive as directly due to the mass (*n*=3, consisting of 2 patients with HOD before surgery and 1 patient who never had surgery or RT), surgery (*n*=3), and surgery and/or RT (*n*=4, HOD after receiving both treatments).

HOD occurs after olivary deafferentation in the Guillain-Mollaret triangle, either from injury to the dentatorubral tract connecting the dentate nucleus to the contralateral red nucleus via the superior cerebellar peduncle, and/or injury to the central tegmental tract connecting the red nucleus to the ipsilateral inferior olive via the brainstem tegmentum [2,7]. A lesion to the efferent limb of the triangle connecting the inferior olive through the inferior cerebellar peduncle to the contralateral dentate nucleus does not result in HOD. The inferior olivary changes occur ipsilateral to tegmental lesions and contralateral to dentate nucleus

lesions, also illustrated with the patients in this study. HOD is usually caused by hemorrhage due to hypertension, with other causes including infarction, surgery, RT, and demyelinating disease [3,4,6–9]. Hemorrhage was only present in four of our patients, suggesting that other space occupying masses and treatments that cause brain tissue destruction may also cause HOD.

HOD is associated with vacuolation of olivary nerve cells caused by trans-synaptic degeneration. Hyperintensity of the olive may occur as early as 3–4 weeks on T2-weighted images, likely due to increased water content and gliosis [2,7]. A meta-analysis by Goyal et al. [2] described increased T2-weighted signal as occurring at 1 month. In our patients who had surgery, HOD was diagnosed a median of 86 days after surgery but as early as 6 days in one patient. We suggest that the increased and more frequent imaging applied today may decrease the observed onset of HOD by reducing length time bias. Swelling occurs 4–6 months after onset from hypertrophic neuronal and astrocytic precursors of cell death and is speculated to result in atrophy after several years [2,7].

Although HOD eventually resolves on imaging after several years, the clinical presentation of palatal myoclonus or palatal tremor with dysrhythmic contractions in the oropharynx, larynx, esophagus, and/or diaphragm persists [4,5]. HOD is commonly found in patients with palatal myoclonus; however, myoclonus is not essential to confirm a diagnosis of HOD [5]. Myoclonus may therefore help support the diagnosis of HOD, but its absence should not dissuade an otherwise confident imaging diagnosis of HOD. We recorded three patients with complaints of dysphagia possibly due to palatal myoclonus, although none underwent formal swallowing evaluation and further conclusions are precluded by the retrospective nature of this study.

Most reports of HOD have described hemorrhagic and ischemic lesions in the posterior fossa as responsible for injury to the Guillain-Mollaret triangle [2–5]. HOD has also been described after posterior fossa tumor resection [6,9]. Unlike the seven posterior fossa tumor patients described by Shinohara et al. [9]; however, 30% of our patients had HOD prior to any brain intervention for their medulloblastoma (n=1), nonspecific cerebellar necrosis (n=1), or demyelination (n=1) (Fig. 1). These tumor and nontumor lesions are postulated to directly damage the Guillain-Mollaret triangle. Precise pathologic destruction is probably required, given that HOD is uncommon with most nonhemorrhagic and nonischemic space occupying mass lesions.

DTI and tractography may be helpful in confirming injury to the Guillain-Mollaret triangle, especially if HOD is suspected [6,10]. Incorporation of diffusion tensor tractography creates a clear visualization of white fiber disruptions within the triangle. Figs. 1 and 2 depict deafferentation causing ipsilateral HOD and contralateral HOD, respectively. In Fig. 1, the superimposed tractography nicely illustrates the truncation of the ipsilateral central tegmental tract, which connects the inferior olive to the ipsilateral red nucleus. In Fig. 2, the tractography confirms thinning and decreased anisotropy of the white fiber tracts in the superior cerebellar peduncle, connecting the left dentate to the contralateral red nucleus.

This study is limited by its retrospective nature and relatively small cohort size. In addition, the time between symptom onset and scan and, therefore, diagnosis were variable in some patients, and between the procedure and follow up scan were variable in other patients. Despite some innate inaccuracies, however, our results suggest that HOD may develop primarily as a result of the mass itself or secondarily as a result of the treatment. Recognizing that there are myriad potential causes, beyond the usual hemorrhagic lesions, is important for the proper diagnosis of HOD. In addition, while T2-hyperintense signal change is in itself nonspecific—with a broad differential of causes such as infection, tumor, and demyelination—the location in the inferior olive and an inciting lesion in the Guillain-Mollaret triangle is highly specific and should allow for a confident imaging diagnosis of HOD in most cases. In conclusion, HOD may develop directly from posterior fossa masses or treatment with surgery and/or RT. Hemorrhage may not be a prominent feature in some cancer and noncancer-related masses. Proper recognition of the characteristic imaging and clinical features is necessary to avoid misdiagnosis of new or recurrent tumor, particularly in cancer patients.

References

1. Gautier JC, Blackwood W. Enlargement of the inferior olivary nucleus in association with lesions of the central tegmental tract or dentate nucleus. Brain. 1961; 84:341–61. [PubMed: 13897315]
2. Goyal M, Versnick E, Tuite P, Cyr JS, Kucharczyk W, Montanera W, et al. Hypertrophic olivary degeneration: metaanalysis of the temporal evolution of MR findings. AJNR Am J Neuroradiol. 2000; 21:1073–7. [PubMed: 10871017]
3. Hornyak M, Osborn AG, Couldwell WT. Hypertrophic olivary degeneration after surgical removal of cavernous malformations of the brain stem: report of four cases and review of the literature. Acta Neurochir (Wien). 2008; 150:149–56. discussion 56. [PubMed: 18166990]
4. Krings T, Foltys H, Meister IG, Reul J. Hypertrophic olivary degeneration following pontine haemorrhage: hypertensive crisis or cavernous haemangioma bleeding? J Neurol Neurosurg Psychiatry. 2003; 74:797–9. [PubMed: 12754356]
5. Phatouros CC, McConachie NS. Hypertrophic olivary degeneration: case report in a child. Pediatr Radiol. 1998; 28:830–1. [PubMed: 9799311]
6. Litkowski P, Young RJ, Wolden SL, Souweidane MM, Haque S, Gilheeney SW. Collision in the inferior olive: hypertrophic olivary degeneration complicated by radiation necrosis in brainstem primitive neuroendocrine tumor. Clin Imaging. 2012; 36:371–4. [PubMed: 22726977]
7. Kitajima M, Korogi Y, Shimomura O, Sakamoto Y, Hirai T, Miyayama H, et al. Hypertrophic olivary degeneration: MR imaging and pathologic findings. Radiology. 1994; 192:539–43. [PubMed: 8029428]
8. Sanverdi SE, Oguz KK, Haliloglu G. Hypertrophic olivary degeneration in children: four new cases and a review of the literature with an emphasis on the MRI findings. Br J Radiol. 2012; 85:511–6. [PubMed: 22337689]
9. Shinohara Y, Kinoshita T, Kinoshita F, Kaminou T, Watanabe T, Ogawa T. Hypertrophic olivary degeneration after surgical resection of brain tumors. Acta Radiol. 2013; 54:462–6. [PubMed: 23486559]
10. Shah R, Markert J, Bag AK, Cure JK. Diffusion tensor imaging in hypertrophic olivary degeneration. AJNR Am J Neuroradiol. 2010; 31:1729–31. [PubMed: 20019104]

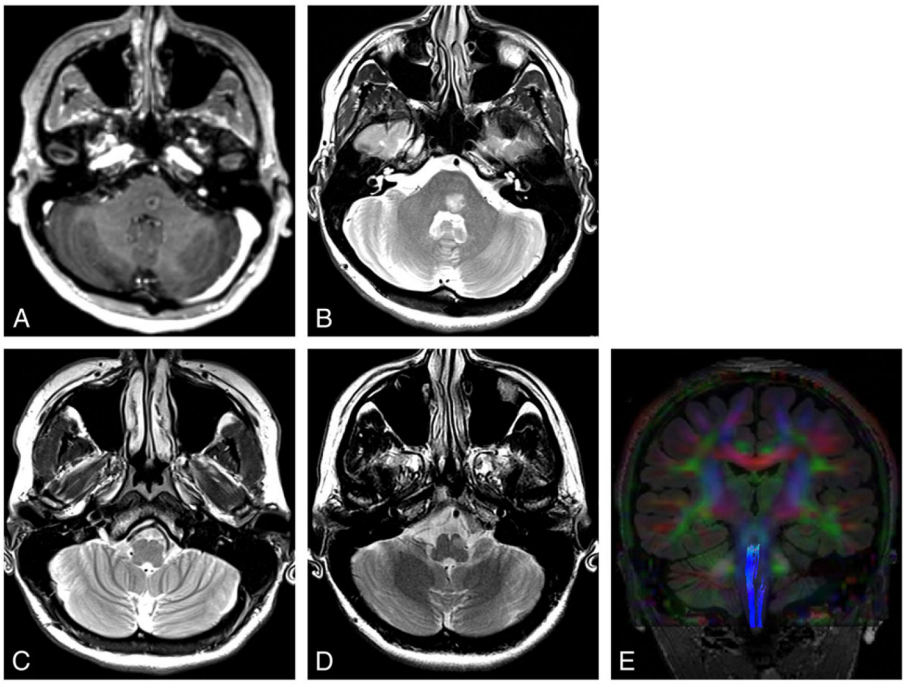

Fig. 1.

Demyelination. Patient presented with horizontal diplopia. Axial contrast T1-weighted image (A) shows a ring enhancing mass in the left paramedian pons. Axial T2-weighted image (B–D) reveals hyperintensity of this demyelinating lesion (B) that decreased over 2 months with steroid treatment (not shown). Image through the inferior olive at presentation (C) shows subtle hyperintensity in the ipsilateral inferior olive consistent with early HOD, with hypertrophy developing 10 months later (D). Tractography superimposed on coronal color FA map (E) shows truncation of the ipsilateral central tegmental tract.

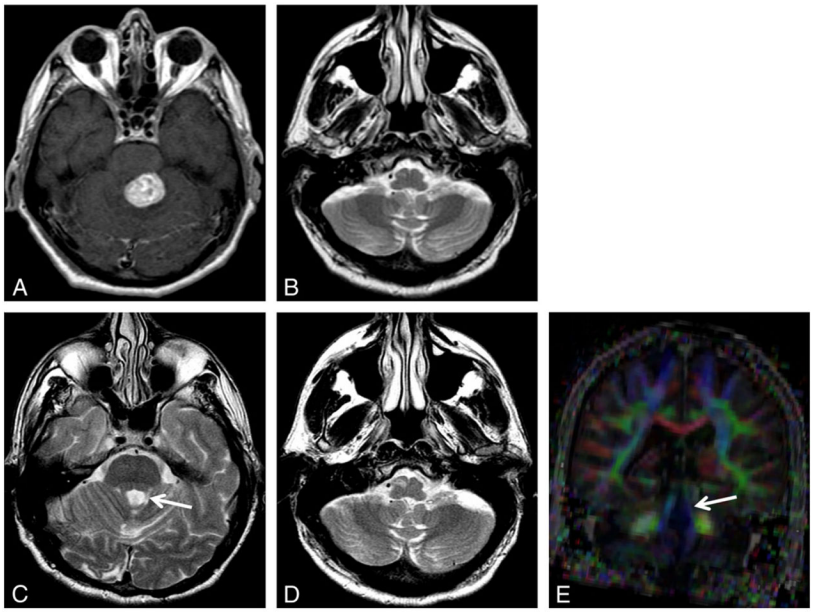

Fig. 2.

Hemangioblastoma. Axial contrast T1-weighted image (A) shows an enhancing hemangioblastoma in the superior left cerebellum. Axial T2-weighted images (B–D): Three months after resection (B), there is new hyperintensity in the contralateral inferior olive. Eight months later, there is atrophy of the superior cerebellar peduncle (C, arrow) and new hypertrophy of the inferior olive consistent with HOD (D). Coronal color FA map (E) confirms thinning and decreased anisotropy of the superior cerebellar peduncle (arrow).

Table 1

Patient characteristics

No.	Age (years)	Sex	Diagnosis	Lesion location	HOD location	Injury to Guillain-Mollaret Triangle	Symptom	Time from lesion detection to HOD (days)	Surgery to HOD (days)	RT to HOD (days)
1	40	M	Medulloblastoma	Cerebellum, midline	Bilateral	Dentate nuclei	Nystagmus	0	–	–
2	46	M	Low grade glioneuronal tumor	Cerebellum, midline	Bilateral	Dentate nuclei	Nystagmus	85	69	–
3	57	M	Hemangio-blastoma	Cerebellum, left	Right	Dentate nucleus	Dysphagia, ataxia	87	86	–
4	53	M	Metastatic renal cortical carcinoma	Cerebellum, left	Right	Dentate nucleus	Nystagmus, ataxia	6	6	–
5	42	M	Medulloblastoma	Cerebellum, midline	Bilateral	Dentate nuclei	Nystagmus	168	97	28
6	28	F	Demyelination	Pons, left	Left	Central tegmental tract	Diplopia	0	–	–
7	46	M	Nonspecific necrosis and histiocytic inflammation	Cerebellum, right	Left	Dentate nucleus	Dsyphagia, nystagmus, ataxia	120	–	–
8	5	F	Primitive neuroectodermal tumor	Pons, right	Right	Central tegmental tract	Ataxia	88	77	28
9	55	F	Anaplastic juvenile pilocytic astrocytoma	Cerebellum, midline	Bilateral	Dentate nuclei	Nystagmus, ataxia	197	197	113
10	67	M	Glioblastoma	Cerebellum, right	Left	Dentate nucleus	Dyphagia, nystagmus	363	363	288